**Classification: biological sciences (plant biology)**

# A novel adaptation of photosynthesis in the marine green alga *Ostreococcus*

Pierre Cardol[1,2,3], Benjamin Bailleul[1,2], Fabrice Rappaport[1,2], Evelyne Derelle[2,4], Daniel Béal[1,2], Cécile Breyton[5], Shaun Bailey[6], Francis André Wollman[1,2], Arthur Grossman[6], Hervé Moreau[2,4], Giovanni Finazzi[1,2*]

[1]Unité Mixte de Recherche 7141 CNRS, Institut de Biologie Physico-Chimique, Paris, France [2]UPMC Université Paris 6, Paris, France [3]Laboratoire de Photobiologie, Département des Sciences la Vie, Université de Liège, Liège, Belgique [4]CNRS, UMR 7628, MBCE, Observatoire Océanologique, F-66651, Banyuls sur mer, France [5]Unité Mixte de Recherche 7099 CNRS, Université Paris7, Institut de Biologie Physico-Chimique, Paris, France [6]The Carnegie Institution, Department of Plant Biology, 260 Panama Street. Stanford University, Stanford CA, USA.

***corresponding author**
Giovanni Finazzi
Institut de Biologie Physico-Chimique
13, rue Pierre et Marie Curie, 75005 Paris – France
Phone : +33 [0]1 58 41 51 01
Fax : +33[0]1 58 41 50 22
giovanni.finazzi@ibpc.fr

ms informations: 21 pages, 5 figures, 1 table, 5 supporting figures, 6115 words, 47198 characters. Abstract: 202 words

Abbreviations: DBMIB, 2,5-dibromo-3-methyl-6-isopropyl-*p*-benzoquinone; Chl, chlorophyll ; DCMU, 3-(3',4'-dichlorophenyl)-1,1-dimethylurea ; E, einstein: moles of photons ; ECS, electrochromic shift ; pgal, propylgallate ; PS, photosystem

**Abstract**

Adaptation of photosynthesis in the marine environment has been examined in two strains of the green, picoeukaryote *Ostreococcus*: OTH95, a surface/high-light strain, and RCC809, a deep-sea/low-light strain. Differences between the two strains include changes in the light harvesting capacity, which is lower in OTH95, and in the photoprotection capacity, which is enhanced in OTH95. Furthermore, RCC809 has a reduced maximum rate of $O_2$ evolution, which is limited by its decreased photosystem (PS) I level, a possible adaptation to Fe limitation in the open oceans. This decrease is, however, accompanied by a substantial rerouting of the electron flow to establish a $H_2O$ to $H_2O$ cycle, involving PSII and a potential plastid plastoquinol terminal oxidase. This pathway bypasses electron transfer through the cytochrome $b_6f$ complex, and allows the pumping of "extra" protons into the thylakoid lumen. By promoting the generation of a large ΔpH, it facilitates ATP synthesis and non-photochemical quenching when RCC809 cells are exposed to excess excitation energy. We propose that the diversion of electrons to oxygen downstream of PSII, but prior to PSI, reflects a common and compulsory strategy in marine phytoplankton, to bypass the constraints imposed by light and/or nutrient limitation, and allow successful colonization of the open-ocean marine environment.

## INTRODUCTION

Picoplankton is defined as unicellular organisms with a cell-size of 0.2 to 3 μm (1). Studies relating to the ecology of this group have greatly expanded over the last decade, and suggest that these tiny organisms play major roles in biogeochemical cycling in the oceans, especially in oligotrophic areas (1). Picoplankton communities contain both prokaryotic and eukaryotic organisms that can be either heterotrophic or autotrophic. Although picoeukaryotes are a minor component of picoplankton communities with respect to cell number, they are major contributors to the primary productivity in coastal areas (1, 2). Within picoeukaryotes, the smallest known organism belongs to the genus *Ostreococcus* (Prasinophyceae, Mamiellales). This genus has a cosmopolitan distribution, and several strains have been isolated or detected in samples of diverse geographical origins (3). The genome of two of these strains have been sequenced recently (4, 5). *Ostreococcus tauri* OTH95 was the first characterized strain, isolated in 1995 from a coastal Mediterranean lagoon in France (6, 7). It is a naked, non-flagellated cell with a single mitochondrion and chloroplast. The chloroplast has simple structural features relative to that of plants; it is reduced in size with only three layers of stacked thylakoid membranes (7). Furthermore, while genes encoding LHCI and prasinophyte-specific chlorophyll-binding proteins ("LHCP") are present in the *Ostreococcus tauri* OTH95 genome, the LHCII genes are absent (8, 9).

Since the description of this first strain, several morphologically indistinguishable *Ostreococcus* isolates originating from surface or deep waters have been established in culture. By analogy with the prokaryotic cyanobacterium *Prochlorococcus* (10, 11), these strains have been defined as low- or high-light strains (12). While the low- and high-light *Ostreococcus* strains exhibit differences in their growth characteristics under various light regimes, it is not clear whether these differences reflect long-term adaptations (speciation) or transient acclimation processes. Furthermore, there is little information concerning the photosynthetic properties of *Ostreococcus*; these properties would strongly influence growth characteristics and the ecological niche in which these organisms could thrive.

Here we show that photosynthesis in *Ostreococcus* has been largely and constitutively shaped by the environment, as evidenced by the comparison between the surface/high-light strain *Ostreococcus tauri* OTH95, and the deep/low-light oceanic strain *Ostreococcus* RCC809. In the former, photosynthesis is very similar to that observed in plants and freshwater algae. Conversely RCC809 is prone to over-reduction of the photosynthetic chain due to the increased light absorption and diminished electron flow capacity as a consequence of reduced cellular PSI content. This leads to increased photosensitivity, which is actively counterbalanced by a singular photoprotection mechanism that involves bypassing the PSI limitation by establishing a $H_2O$ to $H_2O$ cycle: a substantial fraction of PSII-generated electrons are rerouted to oxygen, thank to the activity of a plastoquinol terminal oxidase-like enzyme operating upstream of the cytochrome $b_6f$ complex.

## RESULTS

**The low-light/deep-sea RCC809 strain of *Ostreococcu*s exhibits a reduced ability to acclimate to high light intensities.** The surface/high-light strain *Ostreococcus tauri* OTH95 was the first strain described in the genus (6, 7) and its genome was recently sequenced (4). The *Ostreococcus* deep/low-light strain RCC809 was isolated at 105 meters depth from the tropical zone of the Atlantic ocean. Although the two strains show similar morphological features, they belong to different clades according to their ribosomal RNA sequences. Moreover, they show different growth capacities under high irradiance (12). Both *Ostreococcus* strains can sustain growth for 4 d under light intensities of 10-100 µE $m^{-2}$ $s^{-1}$ (12) (Fig. 1). However, we observed a strong photosensitivity in the deep sea RCC809 strain (Fig. 1B). While this strain is still viable after 4 d at 100 µE $m^{-2}$ $s^{-1}$, the cells could not be rejuvenated after 8-10 d at 100 µE $m^{-2}$ $s^{-1}$ (not shown), suggesting that sustained exposure to this light intensity is above the acclimation threshold of RCC809 (see *e.g.* 13 for further discussion). In contrast, the OTH95 surface strain grew well at 100 µE $m^{-2}$ $s^{-1}$ (Fig. 1B).

We compared the functional properties of each strain after growth under conditions close to those prevailing in their natural environment:

RCC809 cells were grown at 10 μE $m^{-2}$ $s^{-1}$ of blue light, while 100 μE $m^{-2}$ $s^{-1}$ of white light was used for OTH95. These light environments supported near optimal growth rates for each strain. The strains were also switched to the opposite growth light to distinguish between acclimation and adaptation processes that have prevailed for their selection in their natural environment. Cultures were maintained for at least 3 d under the chosen light conditions before photosynthesis was measured.

**PSII absorption capacity is enhanced in RCC809.** Changes in the PSII absorption capacity are typically observed during acclimation of plants and algae to changing light conditions (*e.g.* 14, 15). Although the absorption spectra of RCC809 and OTH95 were similar, we observed a larger contribution of Chl *b* in the overall absorption in the low light/ deep-sea strain (Fig. 2A), suggesting that the relative amount of light harvesting complexes (*i.e.* the ones containing Chl *b*) was larger in the low light- than in the high light-adapted strain. The difference in pigment content was confirmed by the HPLC analysis of the pigments extracted from whole cells. RCC809 was found to have a ~50% higher Chl *b*/*a* ratio than OTH95 (Table 1). Furthermore, the difference in the PSII antenna size was confirmed by measuring the rate of the fluorescence rise under limiting light excitation in the presence of the PSII inhibitor DCMU. In RCC809 the PSII antenna size was increased by a factor of ~1.5 relative to OTH95 under all growth light conditions (Fig. 2B and Fig. S1). This suggests that at least under the conditions explored here, the different PSII antenna content in the two strains does not reflect a reversible acclimation process, but rather a constitutive adaptation to their natural light environments.

**Reduced electron flow from PSII to PSI in RCC809 is compensated for by an increased electron flow to oxygen**. In addition to changes in the size of the light harvesting apparatus, photosynthetic organisms modify the stoichiometry of their reaction centers in response to light and nutrient levels (*e.g.* 14-18). We tested this possibility by quantifying the fraction of active PSI and PSII centers in the two *Ostreococcus* strains. This was done through monitoring the electrochromic shift signal (ECS), a technique previously used to evaluate the PSI/PSII ratio in freshwater green algae (*e.g* 19). The ECS is triggered by the light-

induced electric field that develops across the thylakoid membrane upon charge separation within the reaction centers of the two photosystems. The field modifies the spectrum of pigment-containing complexes due to the Stark effect (20). When illuminated, both *Ostreococcus* strains display an identical ECS signal characterized by more symmetric and sharper peaks than those observed in plants (Fig. S2A,B). These features likely reflect the specific carotenoid composition of the antenna complex LHCP of Mamiellales (8), and the different protein environment of the chromophores (21).

As a prerequisite to the determination of PSI/PSII ratios, we established that the amplitude of the ECS signal was a linear function of the number of light-induced charge separations (Fig. S3). We then assessed the reaction center stoichiometry from the amplitude of the signal measured in cells that were dark adapted for at least four hours before being exposed to a single turnover flash of saturating intensity. Under these conditions, the amplitude of the fast ECS (100µs) is proportional to the photochemical activity of both PSI and PSII and does not depend on either the relative absorption cross section of the PS's (since the flash intensity is saturating), or on the rate of the intersystem electron flow (because the absorption changes are measured before intersystem electron transfer occurs, 20). The relative contribution of PSII was calculated from the difference between the signal measured in the absence and presence of the PSII inhibitors DCMU and hydroxylamine (19). Conversely, the PSI contribution was estimated as the amplitude of the signal that was insensitive to these inhibitors. The PSI/PSII stoichiometry was ~1.4 in OTH95 and ~0.4 in RCC809. This difference reflects a marked decrease in the PSI signal in RCC809 relative to OTH95 (Table I), compared on a Chl basis. These stoichiometries were preserved in each strain independent of the light intensity at which the cells were grown. (Fig. S2 C,D), suggesting that the differences in reaction center stoichiometry between the two strains reflect an adaptation to natural environments in which the strains grow.

To determine the consequences of the decreased PSI/PSII stoichiometry observed in RCC809 on its overall photosynthetic capacity, we measured the light saturation curves of oxygen evolution for both

strains. Maximum oxygen evolution ($P_{max}$) was attained at lower light intensities for RCC809 than for OTH95. Thus RCC809 is capable of maintaining efficient photosynthesis at limiting light, despite the reduced amount of PSI. Conversely, $P_{max}$ was twice as large for OTH95 (215±17 μmoles $O_2$.$h^{-1}$.mg $Chl^{-1}$) relative to RCC809 (104±6 μmoles $O_2$.$h^{-1}$.mg $Chl^{-1}$) once the values were normalized to the Chl concentration (Fig. 3A and Fig. S4). This suggests that the light saturated rate of electron flow from $H_2O$ to $CO_2$ was limited by the decreased PSI content in RCC809. The reduced photosynthetic activity in RCC809 was accompanied by a decrease in the quantum yield of linear electron flow as measured by the fluorescence parameter ΦPSII (22) (Fig. 3B). However, the relative decrease in ΦPSII in RCC809 was much smaller than the overall drop in the rate of oxygen evolution. Such a difference was unexpected as, in principle, both parameters should equally reflect the efficiency of electron flow. However, this result would be predicted if there were an "alternative" electron flow downstream of PSII, and, in particular, a sustained electron transfer from PSII to molecular oxygen. Several alternative electron sinks exist in the chloroplast that utilize $O_2$ as the terminal electron acceptor. They may operate either downstream of PSI (*e.g.* the Mehler reaction, 23) or between PSII and PSI. The latter is the case for the plastoquinol terminal oxidase (PTOX, 24), an enzyme that catalyses electron flow from reduced plastoquinol to $O_2$ during the so-called chlororespiratory process (reviewed in 25). Either the Mehler reaction or the PTOX activity could promote a $H_2O$ to $H_2O$ cycle that would lead to a decrease in the net oxygen evolution yield, without affecting the quantum yield of PSII as evaluated from the fluorescence parameter ΦPSII.

Genes encoding PTOX homologues are present both in OTH95 (CAL55767 and CAL58090) and in RCC809 (Moreau, unpublished). Thus, we tested the possible involvement of PTOX (or a PTOX-related activity) in diverting PSII-generated electrons to molecular oxygen. This was done by measuring the effect of propylgallate (pgal, a known inhibitor of PTOX, *e.g.* 26) on both oxygen evolution and ΦPSII in the two strains. Even at a relatively low concentration (100 μM), this inhibitor strongly decreased the

ΦPSII value of RCC809, consistent with the occurrence of electron flow to molecular oxygen catalyzed by PTOX (Fig. 3C). As expected, pgal only slightly increased the yield of oxygen evolution in this strain: indeed, a $H_2O$ to $H_2O$ cycle will stimulate oxygen emission by PSII, but this rise is strictly compensated by $O_2$ consumption by PTOX. Thus, in the presence of pgal and on a Chl basis, as expected, both oxygen evolution and ΦPSII are reduced by half in RCC809 when compared to OTH95.

There was no major effect of pgal on ΦPSII or oxygen evolution in OTH95, suggesting *i*) that the $H_2O$ to $CO_2$ electron flow is the main pathway for PSII-driven electron flow in this strain, and *ii)* that pgal addition does not result in a specific inhibition of photosynthesis in *Ostreococcus*, at least under the conditions used in our studies.

**A $\Delta\mu_H^+$ is generated in a cytochrome $b_6f$/PSI-independent manner in the RCC809.** As a consequence of the $H_2O$ to $H_2O$ cycle in RCC809 - mediated by PSII and PTOX or a PTOX-like enzyme - one expects at least a fraction of the light-generated electrochemical proton gradient to be established independent of electron flow downstream of the plastoquinone pool (*i.e.* of PSI activity). Indeed, the combined oxidation of water by PSII and of plastoquinol by the oxidase results in a vectorial transfer of $H^+$ from the stroma to the luminal space (*e.g.* 25). This possibility was evaluated by measuring the inversion of the ECS at the end of continuous illumination (27). Inversion of the membrane potential upon switching the light off is assumed to stem from fast $H^+$ flux from the $CF_0/F_1$ ATP synthase complex. Owing to the low dielectric constant of the thylakoid membranes (28), the high $H^+$ buffering capacity of the lumen (29), and to the slow rate of charge redistribution along the membranes (27), the relaxation of the electric component (ΔΨ) of the $\Delta\mu_{H+}$ becomes faster than the complete dissipation of the ΔpH. This leads to a transient excess of positive charges in the stroma, which inverts the membrane potential. Thus, the amplitude of the inverted membrane potential can be taken as an indication of the size of the light induced ΔpH (30). Although this parameter provides only a qualitative estimation of the ΔpH *in vivo*, the values obtained support the notion that RCC809 maintains a lower ΔpH than

OTH95 under our experimental conditions (Fig. 4 and Fig. S5). In addition, while inhibition of PSII activity with DCMU completely abolished the generation of a ΔpH in both strains, a fraction of this proton gradient was maintained in RCC809 cells (but not in OTH95) when electron flow was blocked by addition of the cytochrome $b_6f$ inhibitor DBMIB (scheme I). Further addition of pgal completely suppressed residual electrochemical proton gradient generation, consistent with this "extra" ΔpH being linked to the activity of a PTOX-like oxidase that mediates a $H_2O$ to $H_2O$ cycle.

The fact that an unusual mode of ΔpH generation takes place in RCC809 through a PSII/PTOX-like oxidase-coupled electron flow probably accounts for the different photoprotective responses observed in the two strains. While non-photochemical dissipation of absorbed energy (NPQ, 31) could readily occur in OTH95 in high light, independent of the growth conditions (Table I), NPQ could be observed in RCC809 only upon exposure of the cells to 100 µE $m^{-2}$ $s^{-1}$ for several days. This NPQ was paralleled by accumulation of antheraxanthin (Table I, the only product of violaxanthin deepoxidation in Prasinophytes, *e.g.* 32), as expected if the "extra" PTOX-dependent ΔpH generated at this light may sustain a greater activity of violaxanthin deepoxidase (31) in RCC809.

## DISCUSSION

Despite their identical morphology, the two *Ostreococcus* strains characterized in this work - OTH95 and RCC809 (12) - display distinct photosynthetic traits that have been shaped by their contrasting growth environments. OTH95 strain was isolated in the Thau coastal lagoon in western Mediterranean, *i.e.* a rather shallow environment rich in nutrients, often subjected to strong illumination (especially in the summer time). In contrast, RCC809 is an oceanic strain, isolated in the deep sea (~ 100 m depth), where it will not encounter light stress, but is likely subjected to nutrient limitation (*e.g.* Fe). The most striking feature observed in our analysis is the water-to-water cycle generated by PSII in RCC809 but not in OTH95. We characterized this process, specific to RCC809, as a PTOX-mediated electron sink based on two independent observations: *i)* the

inhibition of the quantum yield of PSII-driven electron flow (ΦPSII) by pgal, without any effect on the oxygen evolution capacity, and *ii)* the generation of a ΔpH in the light under conditions in which electron flow is blocked at the level of the cytochrome $b_6f$ complex (by DBMIB). Generation of this "extra" ΔpH, is inhibited by blocking electron flow at the level of PSII by DCMU, or by adding pgal at a concentration that inhibits ΦPSII.

Alternative electron flow to oxygen is prominent in RCC809; ~50% of the electrons generated from water oxidation can be routed to the reduction of molecular oxygen, at the cost of $CO_2$ fixation. No such sustained activity of a water-to-water cycle has been observed in vascular plants or freshwater green algae (25, 33). However, an important rerouting of photosynthetic electrons to molecular oxygen has been shown in marine prokaryotes under nutrient-replete conditions (34) or *in situ* where the organisms may be experiencing nutrient limitation (35). It is thus conceivable that this phenomenon represents a typical response of organisms adapted to life in the nutrient-poor oligotrophic oceans.

What then is the rationale for such an adaptation mechanism? Previous work has emphasized that algae and plants respond to environmental changes by modulating the size of their light harvesting complexes as well as the stoichiometry of their reaction centers (13-16, 36-40). However, while the changes in the antenna size of RCC809 are consistent with this organism being adapted to a low light environment, the low PSI/PSII ratio in this strain is typical of high light-acclimated plants (14). It is thus tempting to speculate that the situation observed in RCC809 reflects a constitutive adaptation to a sustained nutrient limitation (*e.g.* Fe) experienced by this strain. Owing to its relatively high Fe content, PSI is strongly decreased in freshwater (17) or marine (18) algae that are exposed to a Fe-deplete environment. Independent of the origin of the large decrease in the PSI content observed in RCC809, the unusually high activity of the PTOX-like oxidase may be essential for this strain to survive, even at moderate light intensities. The concomitant increase in light harvesting capacity of PSII and the decrease in PSI cellular content would rapidly

promote over-reduction of the plastoquinone pool, eventually leading to sustained photodamage, would this strain be subjected to higher light. However, this potential lethal situation is actively counterbalanced in RCC809 by the oxidase-mediated water-to-water cycle. By acting as an efficient electron sink, this process allows reoxidation of the electron transport components, and the opening of PSII traps. Consistent with this hypothesis, RCC809 is capable of maintaining a partially oxidized electron transport chain even at light intensities where electron flow to $CO_2$ is limited by PSI performances (Fig. 3).

Furthermore, by bypassing the bottleneck step of electron transfer through PSI, this process has a major advantage when compared to electron flow to other alternative sinks (*i.e*. the Mehler reaction or the transfer of reducing equivalents to the mitochondria *via* the malate-shunt, 41), which require activity of both photosystems. The water-to-water cycle also provides other benefits to the cell: *i)* by allowing the development of a ΔpH-mediated NPQ response it enhances photoprotection. Previous work has demonstrated that the ΔpH activates the VDE enzyme (responsible for antheraxanthin and zeaxanthin synthesis), leading to an enhanced thermal dissipation capacity (reviewed in 31). Thus, the "extra" ΔpH generated in RCC809 may be responsible for the accumulation of antheraxanthin that is observed after several days of exposure to 100 µE $m^{-2}$ $s^{-1}$. This antheraxanthin promotes the onset of reversible fluorescence quenching, which may prolong viability of RCC809 during extended periods in high light. Moreover *ii)* the "extra" ΔpH can fuel ATP synthesis for housekeeping purposes, even in the presence of reduced PSI performances. It is known from previous work in plants and algae that electron diversion at the PSI acceptor side (*via* the Mehler reaction, the malate shunt, or cyclic flow around PSI) may increase the amount of ATP synthesized per electron transferred in PSII. This likely allows establishing the correct ATP/NADPH ratio as required for $CO_2$ assimilation by the Calvin-Benson cycle (see *e.g.* 42 for a discussion). In analogy to the cyclic electron flow observed around PSI, activation of a water-to-water cycle around PSII -under nutrient starvation, and/or any other condition leading a significant drop in the PSI

levels - may increase the ATP synthesized per electron transferred in PSI and help sustaining cell survival. Furthermore, although this process was observed under controlled laboratory conditions, a comparison with previous observations in diatoms and cyanobacteria (*e.g.* 18, 34) suggests that electron diversion downstream of PSII may be widespread among the prokaryotic and eukaryotic components of phytoplankton. Thus we propose that rerouting of electrons to a plastoquinol oxidase represents a common and compulsory strategy to allow successful adaptation of photosynthetic taxa to the oligotrophic ocean environment.

## MATERIAL AND METHODS

**Growth conditions.** *Ostreococcus* OTH95 (*O. tauri*, 7) and RCC809 strains were obtained from the Observatoire Océanologique de Banyuls-sur-Mer, France and grown in K medium (43). They were grown either in white light at an intensity of 100 µE $m^{-2}$ $s^{-1}$ or in blue light at an intensity of 10 µE $m^{-2}$ $s^{-1}$ (filter 183 Moonlight Blue Filter, Leefilters, UK) in a 12 h light/12 h dark regime at 18-20°C with mild agitation. This temperature represents a compromise between the range experienced by OTH95 (20-25°C) and RCC809 (15-20°C) in their natural environments (see *e.g.* http://bulletin.mercator-ocean.fr). Flow cytometric analyses were performed with a FACScan flow cytometer (Becton Dickinson, San Jose, CA, USA) equipped with an air-cooled argon laser providing 15 mW at 488 nm.

**Fluorescence and oxygen measurements.** Fluorescence emission was measured using a home-built instrument, as described (44). ΦPSII, the quantum yield of PSII (22), was calculated as (Fm'-Fs)/Fm', where Fm' is the maximum fluorescence emission level induced by a pulse of saturating light (~ 5000 µE $m^{-2}$ $s^{-1}$) and Fs is the steady state level of fluorescence emission. NPQ was calculated as (Fm-Fm')/Fm' (45), where Fm is the maximum fluorescence emission level in the dark measured with the saturating pulse of light. The ΔpH-sensitive NPQ extent was evaluated as the fraction of fluorescence quenching that was selectively suppressed by addition of the $H^+/K^+$ exchanger nigericin (10 µM). Oxygen evolution was measured with a Clark electrode (Hansatech, UK).

**Spectroscopic measurements.** *In vivo* absorption was measured with a home-built spectrophotometer, based on a detecting diode array (AVS-USB 200, Ocean Optics, USA). Kinetics measurements were performed using a home-built xenon-lamp-based spectrophotometer (19). Detection flashes were provided by a xenon flashlamp (3 $\mu$s duration at half-height) with light filtered through a monochromator (HL, Jobin Yvon, France). Actinic light was provided either by a dye laser or by a continuous green LED source. PSI and PSII charge separation capacity was calculated from changes in the amplitude of the fast phase of the ECS signal (at 505 nm – 525 nm) upon excitation with a saturating laser flash signal in the presence or absence of the PSII inhibitors DCMU (20 µM) and hydroxylamine (1 mM). The latter compound was added to destroy the manganese cluster responsible for oxygen evolution and to prevent recombination between the donor and acceptor side of PSII, which would preclude correct estimation of the PSI/PSII ratio.

**Pigment analysis.** Pigments were extracted from whole cells in methanol and debris was removed by centrifugation at 10,000x *g* for 15 min. 15 µl of pigment extract was subjected to reverse-phase HPLC analysis using a commercial equipment (Waters, Milford, MA). A Nova Pak C18, 60A column (150-mm length, 4-µm pore size) was used for separation. The Chl *a* and *b* concentrations were estimated according to (46).

**Acknowledgements.** We thank Fabrice Franck (Liège) and Bernard Genty (Cadarache) for valuable suggestions. M. Radoux is also thanked for technical assistance. This research was supported by grants from the Belgian "Fonds National de la Recherche Scientifique" (FNRS) (F.4735.06) to PC and from the Centre National de la Recherche Scientifique (CNRS). HM is supported by the "Marine Genomics Europe" European Network of Excellence (2004-2008) (GOCE-CT-2004-505403). SB is supported by NSF grant OCE-0450874, awarded to ARG. PC is a research associate from the Belgian FNRS.

**References**


1. Li WKW (1994) Primary productivity of prochlorophytes, cyanobacteria, and eucaryotic ultraphytoplankton : measurements from cytometric sorting. *Limnol Oceanogr* **39:**169-75.
2. Worden AZ, Nolan JK, Palenik B (2004) Assessing the dynamic and ecology of marine picoplankton : the importance of eukaryotic component. *Limnol Oceanogr* **49:**168-79.
3. Zhu F, Not F, Massana R, Marie D, Vaulot D (2005) Mapping of the picoeukaryotes in marine systems with quantitative PCR of the 18S rRNA gene. *FEMS Microbiol Ecology* **52:**79-92.
4. Derelle E, Ferraz C, Rombauts S, Rouze P, Worden AZ, Robbens S, Partensky F, Degroeve S, Echeynie S, Cooke R, Saeys Y, Wuyts J, Jabbari K, Bowler C, Panaud O, Piegu B, Ball SG, Ral JP, Bouget FY, Piganeau G, De Baets B, Picard A, Delseny M, Demaille J, Van de Peer Y, Moreau H (2006) Genome analysis of the smallest free-living eukaryote Ostreococcus tauri unveils many unique features. *Proc Natl Acad Sci U S A* **103:**11647-52.
5. Palenik B, Grimwood J, Aerts A, Rouze P, Salamov A, Putnam N, Dupont C, Jorgensen R, Derelle E, Rombauts S, Zhou K, Otillar R, Merchant SS, Podell S, Gaasterland T, Napoli C, Gendler K, Manuell A, Tai V, Vallon O, Piganeau G, Jancek S, Heijde M, Jabbari K, Bowler C, Lohr M, Robbens S, Werner G, Dubchak I, Pazour GJ, Ren Q, Paulsen I, Delwiche C, Schmutz J, Rokhsar D, Van de Peer Y, Moreau H, Grigoriev IV (2007) The tiny eukaryote Ostreococcus provides genomic insights into the paradox of plankton speciation. *Proc Natl Acad Sci U S A* **104:**7705-10.
6. Courties C, Vaquer A, Troussellier M, Lautier J, Chrétiennot-Dinet MJ, Neveux J, Machado MC, Claustre H (1994) Smallest eukaryotic organism. *Nature* **370:**255.
7. Chrétiennot-Dinet MJ, Courties C, Vaquer A, Neveux J, Claustre H, Lautier J, Machado MC (1995) A new marine picoeukaryote : *Ostreococcus tauri* gen et sp. Nov. (Chlorophyta, Prasinophyceae). *Phycologia* **4:**285-92.

8. Six C, Worden AZ, Rodriguez F, Moreau H, Partensky F (2005) New insights into the nature and phylogeny of prasinophyte antenna proteins: *Ostreococcus tauri*, a case study. *Mol Biol Evol* **22:**2217-30.
9. Derelle E, Ferraz C, Lagoda P, Eychenié S, Cooke R, Regad F, Sabau X, Courties C, Delseny M, Demaille J, Picard A, Moreau H (2002) DNA librairies for sequencing the genome of *Ostreococcus tauri* (chlorophyta, prasinophyceae) : the smallest free-living eukrayotic cell. *J Phycol* **38:**1150-6.
10. Moore LR, Rocap G, Chisholm SW (1998) Physiology and molecular phylogeny of coexisting *Prochlorococcus* ecotypes. *Nature* **393:**464-7.
11. Rocap G, Distel DL, Waterbury JB, Chisholm SW (2002) Resolution of *Prochlorococcus* and *Synechococcus* ecotypes by using 16S-23S ribosomal DNA internal transcribed spacer sequences. *Appl Environ Microbiol* **68:**1180-91.
12. Rodriguez F, Derelle E, Guillou L, Le Gall F, Vaulot D, Moreau H (2005) Ecotype diversity in the marine picoeukaryote Ostreococcus (Chlorophyta, Prasinophyceae). *Environ Microbiol* **7:**853-9.
13. Walters RG (2005) Towards an understanding of photosynthetic acclimation. *J Exp Bot* **56:**425-47.
14. Anderson JM, Chow WS, Park Y-I (1995) The grand design of photosynthesis: Acclimation of the photosynthetic apparatus to environmental clues. *Photosynth Res* **46:**129-39.
15. Falkowski PG, Owens TG (1980) Light-Shade Adaptation : TWO STRATEGIES IN MARINE PHYTOPLANKTON. *Plant Physiol* **66:**592-5.
16. Bailey S, Walters RG, Jansson S, Horton P (2001) Acclimation of *Arabidopsis thaliana* to the environment: the existence of separate low light and high light responses. *Planta* **231:**794-801.
17. Moseley JL, Allinger T, Herzog S, Hoerth P, Wehinger E, Merchant S, Hippler M (2002) Adaptation to Fe-deficiency requires remodeling of the photosynthetic apparatus. *Embo J* **21:**6709-20.

18. Strzepek RF, Harrison PJ (2004) Photosynthetic architecture differs in coastal and oceanic diatoms. *Nature* **431:**689-92.
19. Joliot P, Delosme R (1974) Flash-induced 519 nm absorption change in green algae. *Biochim Biophys Acta* **357:**267-84.
20. Witt HT (1979) Energy conversion in the functional membrane of photosynthesis. Analysis by light pulse and electric pulse methods. The central role of the electric field. *Biochim Biophys Acta* **505:**355-427.
21. Goss R, Wilhelm C, Garab G (2000) Organization of the pigment molecules in the chlorophyll a/b/c containing alga *Mantoniella squamata* (Prasinophyceae) studied by means of absorption, circular and linear dichroism spectroscopy. *Biochim Biophys Acta* **1457:**190-9.
22. Genty B, Harbinson J, Briantais J-M, Baker NR (1990) The relationship between non-photochemical quenching of chlorophyll fluorescence and the rate of photosystem 2 photochemistry in leaves. *Photosynth Res* **25:**249-57.
23. Ort DR, Baker NR (2002) A photoprotective role for O(2) as an alternative electron sink in photosynthesis? *Curr Opin Plant Biol* **5:**193-8.
24. Streb P, Josse EM, Gallouet E, Baptist F, Kuntz M, Cornic G (2005) Evidence for alternative electron sinks to photosynthetic carbon assimilation in the high mountain plant species *Ranunculus glacialis.* *Plant Cell Environ* **28:**1123-35.
25. Peltier G, Cournac L (2002) Chlororespiration. *Annu Rev Plant Biol* **53:**523-50.
26. Josse EM, Alcaraz JP, Labouré AM, Kuntz M (2003) In vitro characterization of a plastid terminal oxidase (PTOX). *Eur J Biochem* **270:**3787-94.
27. Cruz JA, Sacksteder CA, Kanazawa A, Kramer DM (2001) Contribution of electric field (Δψ) to steady-state transthylakoid proton motive force (pmf) in vitro and *in vivo*. Control of pmf parsing into Δψ and ΔpH by ionic strength. *Biochemistry* **40:**1226-37.

28. Vredenberg WJ (1976) in *The intact chloroplast*, ed. Barber L (Elsevier / North Holland Biomedical press, Amsterdam), pp. 53-87.
29. Junge W, McLaughlin S (1987) The role of fixed and mobile buffers in the kinetics of proton movement. *Biochim Biophys Acta* **890:**1-5.
30. Kramer DM, Cruz JA, Kanazawa A (2003) Balancing the central roles of the thylakoid proton gradient. *Trends Plant Sci* **8:**27-32.
31. Horton P, Ruban AV, Walters RG (1996) Regulation of Light Harvesting in Green Plants. *Annu Rev Plant Physiol Plant Mol Biol* **47:**655–84.
32. Goss R, Böhme K, Wilhelm C (1998) The xanthophyll cycle of *Mantonielle squamata* converts violaxanthin into antheraxanthin but not zeaxanthin : consequences for the mechanism of enhanced non-photochemical energy dissipation. *Planta* **205:**613-21.
33. Cournac L, Redding K, Ravenel J, Rumeau D, Josse EM, Kuntz M, Peltier G (2000) Electron flow between photosystem II and oxygen in chloroplasts of photosystem I-deficient algae is mediated by a quinol oxidase involved in chlororespiration. *J Biol Chem* **275:**17256-62.
34. Bailey S, Melis A, Mackey K, Cardol P, Finazzi G, Dijken G, van Berg GM, Arrigo K, Shrager J, Grossman AR (2008) Alternative photosynthetic electron flow to oxygen in marine Synechococcus. *Biochim Biophys Acta* **doi:10.1016/j.bbabio.2008.01.002**.
35. Behrenfeld MJ, Worthington K, Sherrell RM, Chavez FP, Strutton P, McPhaden M, Shea DM (2006) Controls on tropical Pacific Ocean productivity revealed through nutrient stress diagnostics. *Nature* **442:**1025-8.
36. Demmig-Adams B (1998) Survey of thermal energy dissipation and pigment composition in sun and shade leaves. *Plant Cell Physiol* **39:**474-82.
37. Berry J, Bjorkman O (1980) Photosynthetic response and adaptation to temperature in higher-plants. *Annu Rev Plant Physiol Plant Mol Biol* **31:**491-543.
38. LaRoche J, Mortain-Bertrand A, Falkowski P (1991) Light intensity induced changes in cab mRNA and light harvesting complex II

apoprotein levels in the unicellular chlorophyte *Dunaliella tertiolectica. Plant Physiol* **97:**147-53.

39. Durnford DG, Falkowski PG (1997) Chloroplast redox regulation of nuclear gene transcription during photoacclimation. *Photosynth Res* **53:**229-41.
40. Im CS, Grossman AR (2001) Identification and regulation of high light-induced genes in *Chlamydomonas reinhardtii. Plant J* **30:**301-13.
41. Scheibe R, Backhausen JE, Emmerlich V, Holtgrefe S (2005) Strategies to maintain redox homeostasis during photosynthesis under changing conditions. *J Exp Bot* **56:**1481-9.
42. Allen J (2002) Photosynthesis of ATP-electrons, proton pumps, rotors, and poise. *Cell* **110:**273-6.
43. Keller MD, Selvin RC, Claus W, Guillard RRL (1987) Media for the culture of oceanic ultrphytoplankton. *J Phycol* **23:**633-8.
44. Rappaport F, Beal D, Joliot A, Joliot P (2007) On the advantages of using green light to study fluorescence yield changes in leaves. *Biochim Biophys Acta* **1767:**56-65.
45. Bilger W, Björkman Ö (1990) Role of the xanthophyll cycle in photoprotection elucidated by measurments of light-induced absorbance changes, fluorescence and photosynthesis in leaves of *Hedera canariensis. Photosynth Res* **25:**173-86.
46. Lichtenthaler HK (1987) Chlorophylls and carotenoids: pigments of photosynthetic biomembranes. *Methods enzymol* **148:**350-82.

## FIGURE LEGENDS

**Figure 1. Growth kinetics of OTH95 and RCC809 *Ostreococcus* strains at different light intensities.** The two strains OTH95 (squares) and RCC809 (triangles) were grown at low light (10 µE $m^{-2}$ $s^{-1}$, blue filter, panel A) or moderate/high light (100 µE $m^{-2}$ $s^{-1}$, panel B). Error bars: standard error of the mean of three independent measurements.

**Figure 2. Comparative absorption and fluorescence characteristics of OTH95 and RCC809 strains. A**: Absorption spectrum of intact OTH95 (dashed line) and RCC809 (solid line) cells. Curves were normalized to absorption at 440 nm. **B**: Fluorescence transients of OTH95 (squares) and RCC809 (triangles) in the presence of 20 µM DCMU. Curves were normalized to the same value of variable fluorescence to allow a better comparison. Error bars: standard error of the mean of three independent measurements.

**Figure 3. Light saturation curves of oxygen evolution, ΦPSII and the effect of pgal in OTH95 (squares) and RCC809 (triangles) cells**. **A**: Oxygen evolution was monitored using a Clark electrode under increasing light intensity, adjusted every 2 min. Photosynthetic activity was calculated as "net photosynthesis" (*i.e*. photosynthesis after correction for respiration) at any given light intensity **B**: ΦPSII, calculated as (Fm'-Fs)/Fm' (ΔF/Fm) (22). **C**: effect of pgal on both oxygen evolution and ΦPSII. Values are expressed as a percentage of change with respect to the untreated sample. Error bars: standard error of the mean of three independent measurements.

**Figure 4. Estimation of the electrochemical proton gradient generated upon steady-state illumination in OTH95 (A) and RCC809 (B) cells**. Membrane potential is evaluated by absorption changes at 505-525 nm on untreated cells (black symbols), with 20 µM DCMU (crossed symbols), 5 µM DBMIB (grey symbols), 5 µM DBMIB and 100 µM pgal (open

symbols). Samples were illuminated for 2 min with saturating light (white box). The light was then switched off (black box), and the membrane potential decay was followed until full relaxation. The amplitude of the membrane potential was normalized to 1 PSII membrane charge separation, corresponding to the contribution of PSII to the signal generated by a saturating laser flash (see *e.g.* Fig.s S2 and S3).

**Scheme I:** Photosynthetic electron flow. The site of coupling between electron and proton transfer, as well as the sites of inhibition by DCMU and DBMIB are shown. Activity of PTOX or a PTOX-like oxidase (inhibited by pgal) may allow diversion of electrons from the plastoquinone pool ($PQH_2$) to oxygen, and stimulate proton deposition into the lumen by a DCMU sensitive, DBMIB insensitive reaction. See text for further details.

| | OTH95 | RCC809 |
|---|---|---|
| Chl *b* / Chl *a* | 0.65 ± 0.05 | 1.01 ± 0.08 |
| PSI | 1.41 ± 0.15 | 0.42 ± 0.2 |
| PSII | 1 | 1.08 ± 0.22 |
| $\frac{PSI}{PSII}$ | 1.41± 0.15 | 0.39 ± 0.08 |
| $NPQ_{10\mu E}$ | 1.53 ± 0.47 | 0.09 ± 0.07 |
| $NPQ_{100\mu E}$ | 1.65 ± 0.35 | 0.75 ± 0.16 |
| $\frac{Ax}{Ax+Vx}^{10\mu E}$ | 0.01± 0.001 | 0.01 ± 0.003 |
| $\frac{Ax}{Ax+Vx}^{100\mu E}$ | 0.04 ± 0.01 | 0.210 ± 0.026 |

**Table 1. Photosynthetic parameters of the *Ostreococcus* strains OTH95 and RCC809.** Chl *b*/*a* ratios were estimated by HPLC pigment analysis of light-adapted cells. The high cellular Chl *b/a* value is attributable to an elevated cellular content of LHCP, which has a very high Chl *b/a* ratio (~ 1.3) (8, 12). ΔpH-induced NPQ was calculated as the nigericin sensitive fraction of steady state fluorescence quenching (Fm-Fm'/Fm'), which was induced by exposure of cells grown at 10 or 100 µE $m^{-2}$ $s^{-1}$ of saturating illumination (45). PSI/PSII ratios were estimated from PSI and PSII charge separation capacity. Values were normalized to Chl concentrations, and the value for PSII centers in OTH95 (100 µE $m^{-2}$ $s^{-1}$) was arbitrary set to 1. Ax/(Ax+Vx) is the deepoxidation state of xanthophylls. Standard errors are relative to at least three replicate experiments.

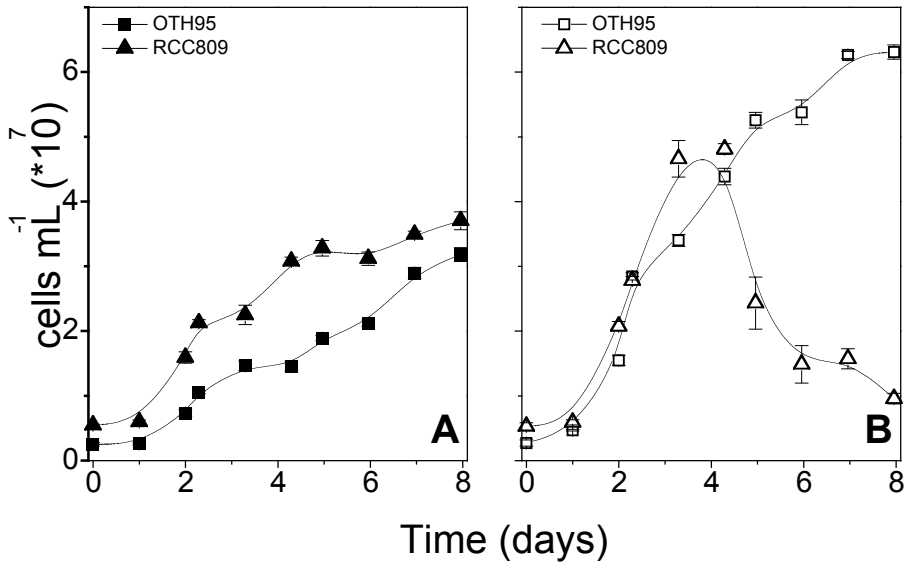


Fig. 1

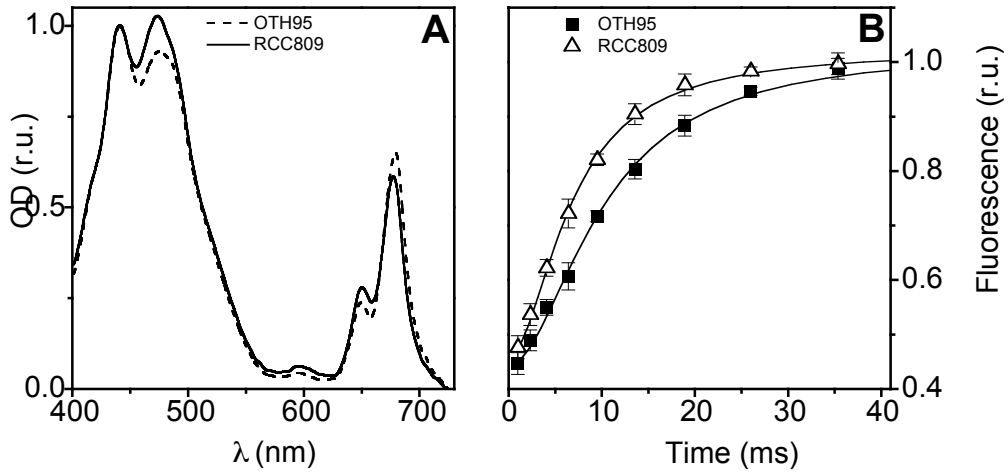
A
OTH95
RCC809
1.0
0.5
0.0
OD (r.u.)
400
500
600
700
λ (nm)
B
OTH95
RCC809
1.0
0.8
0.6
0.4
Fluorescence (r.u.)
0
10
20
30
40
Time (ms)

Fig. 2

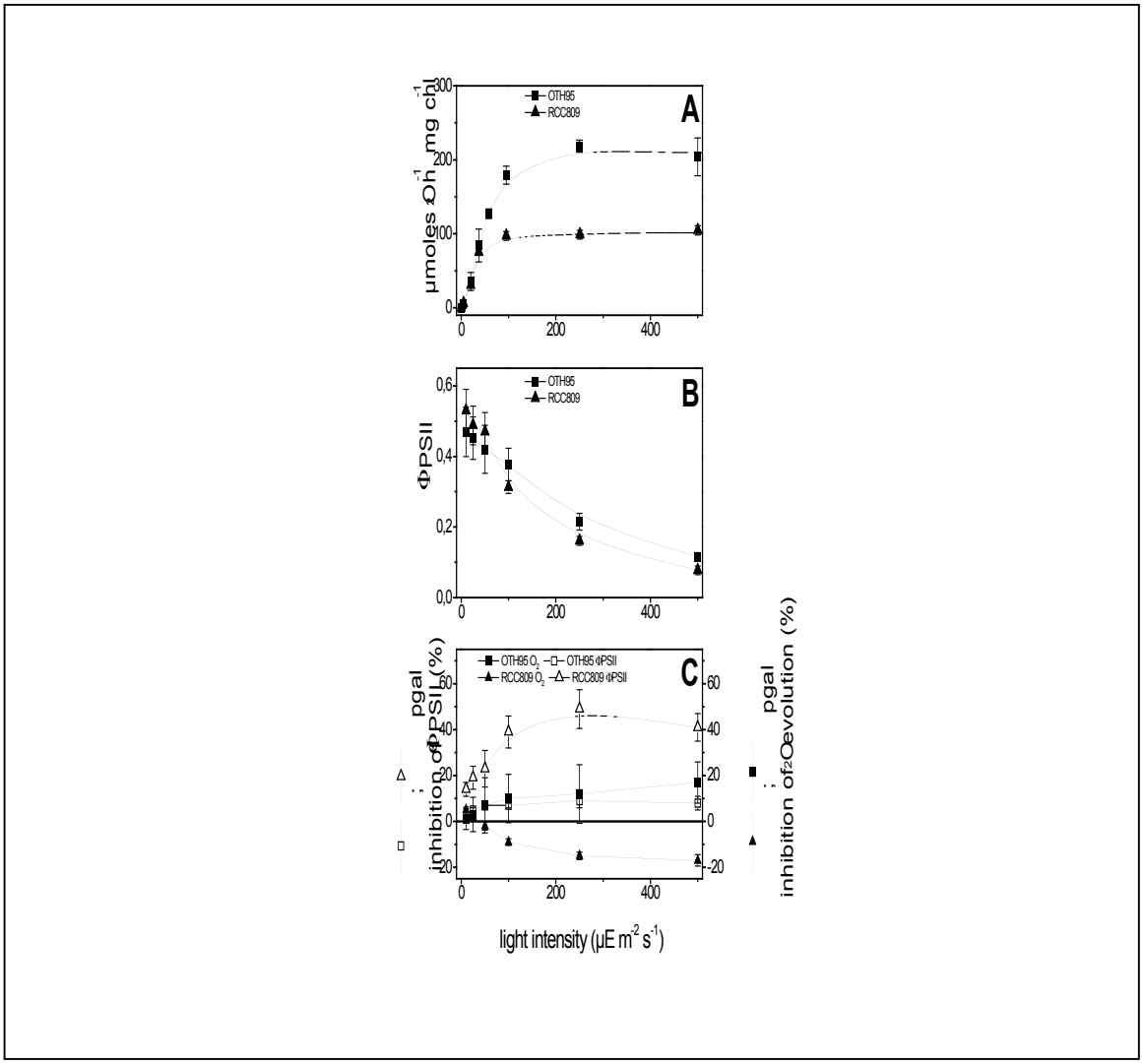
A
OTH95
RCC809
µmoles O2 mg chl-1
B
ΦPSII
C
OTH95 O2
OTH95 ΦPSII
RCC809 O2
RCC809 ΦPSII
pgal ; ΦPSII (%)
pgal ; inhibition of O2 evolution (%)
light intensity (µE m-2 s-1)

Fig. 3

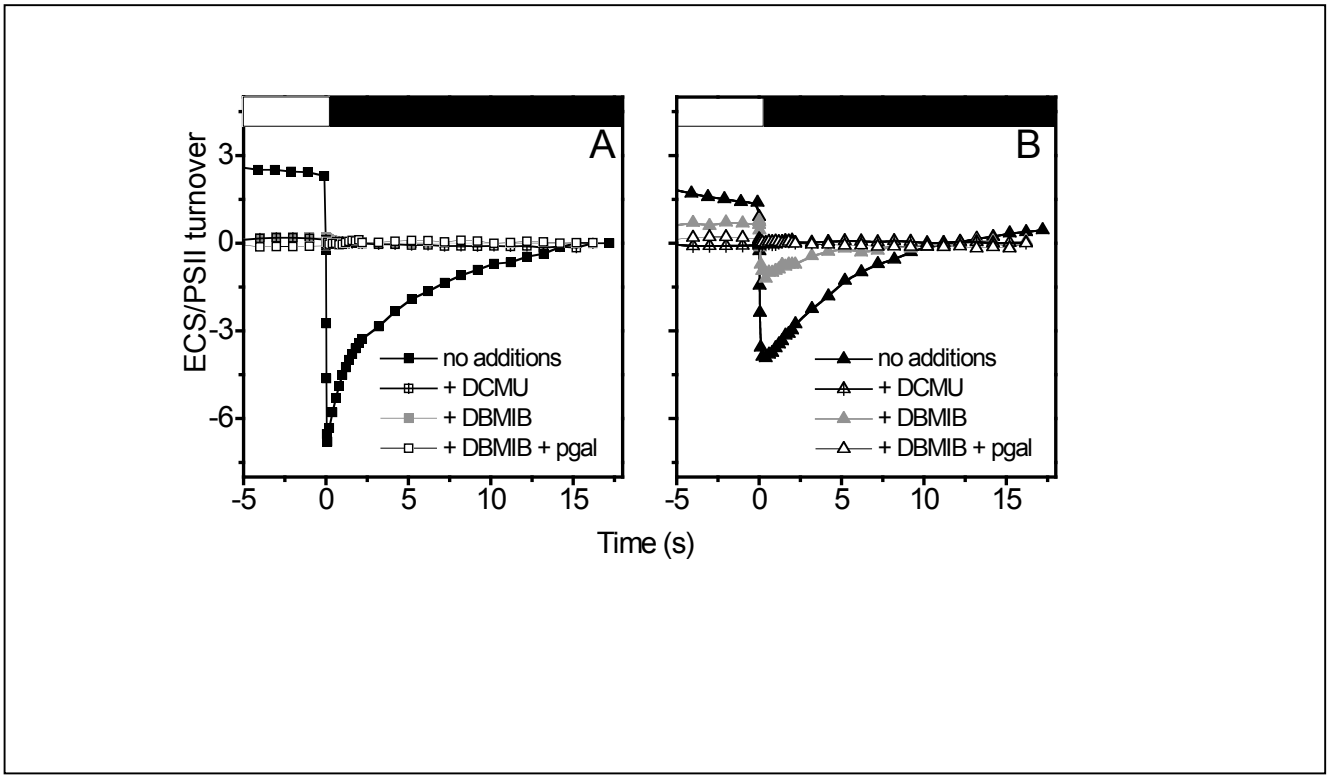
A
B
ECS/PSII turnover
3
0
-3
-6
-5
0
5
10
15
Time (s)
no additions
+ DCMU
+ DBMIB
+ DBMIB + pgal

Fig. 4

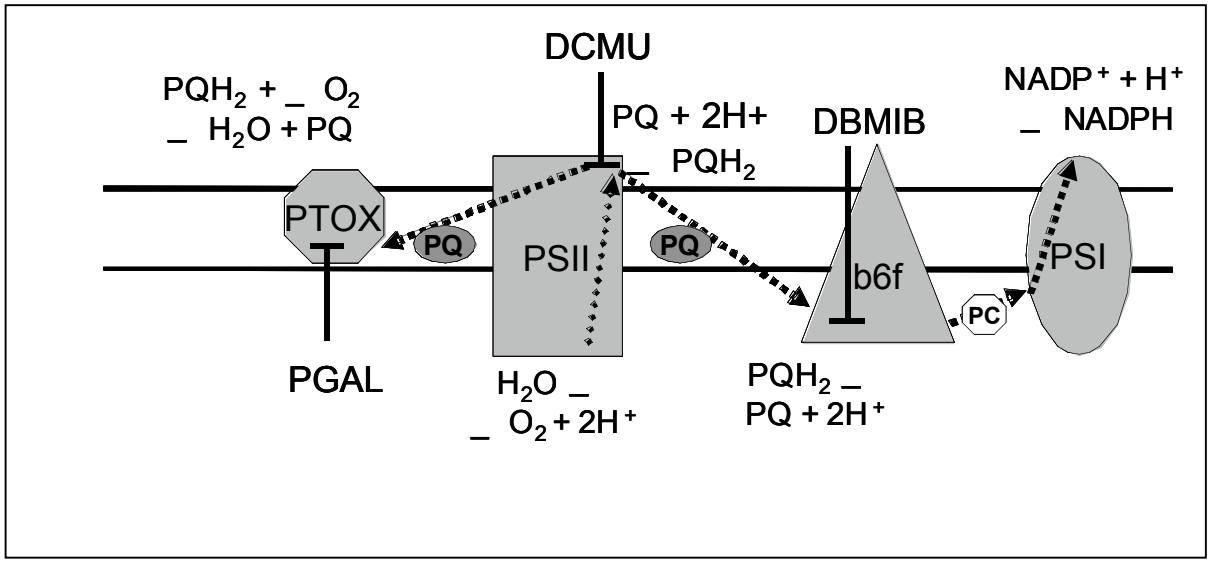
DCMU
PQH2 + _ O2
_ H2O + PQ
PQ + 2H+
_ PQH2
DBMIB
NADP+ + H+
_ NADPH
PTOX
PQ
PSII
PQ
b6f
PC
PSI
PGAL
H2O _
_ O2 + 2H+
PQH2 _
PQ + 2H+

Scheme I

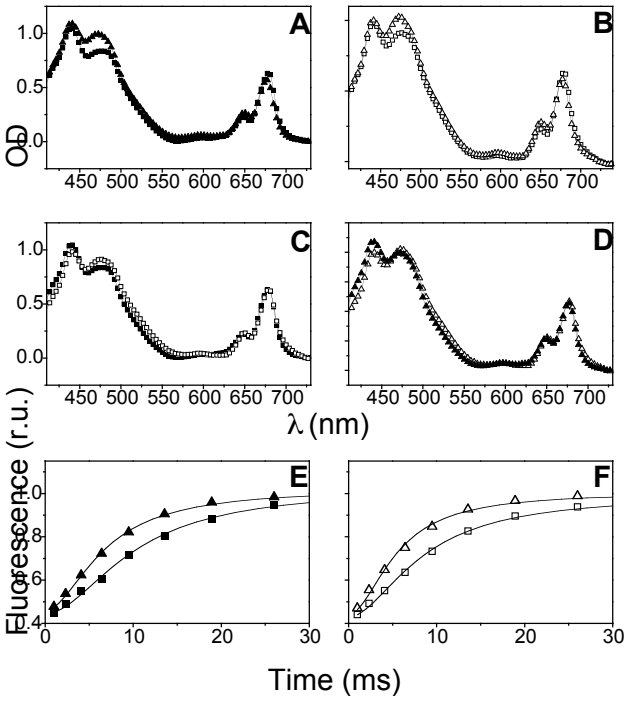


**Figure S1 online. Comparative absorption and fluorescence characteristics of OTH95 (squares) and RCC809 (triangles) strains. A-D**: Absorption spectrum of intact cells. Spectra were normalized on the absorption at 440 nm. **E** and **F:** Fluorescence transients of OTH95 and RCC809 cells in the presence of 20 μM DCMU. Traces were normalized to the same value of variable fluorescence to allow a better comparison. **A**, **E**: cells were grown at 100 μE $m^{-2}$ $s^{-1}$ of white light; **B**, **F**: cells were grown at 10 μE $m^{-2}$ $s^{-1}$ of blue light. **C:** comparison between the spectra measured in OTH95 cells grown at 10 μE $m^{-2}$ $s^{-1}$ (open squares) and 100 μE $m^{-2}$ $s^{-1}$ (solid squares) **D.** Comparison between the spectra measured in RCC809 cells grown at 10 μE $m^{-2}$ $s^{-1}$ (open triangles) and 100 μE $m^{-2}$ $s^{-1}$ (solid triangles).

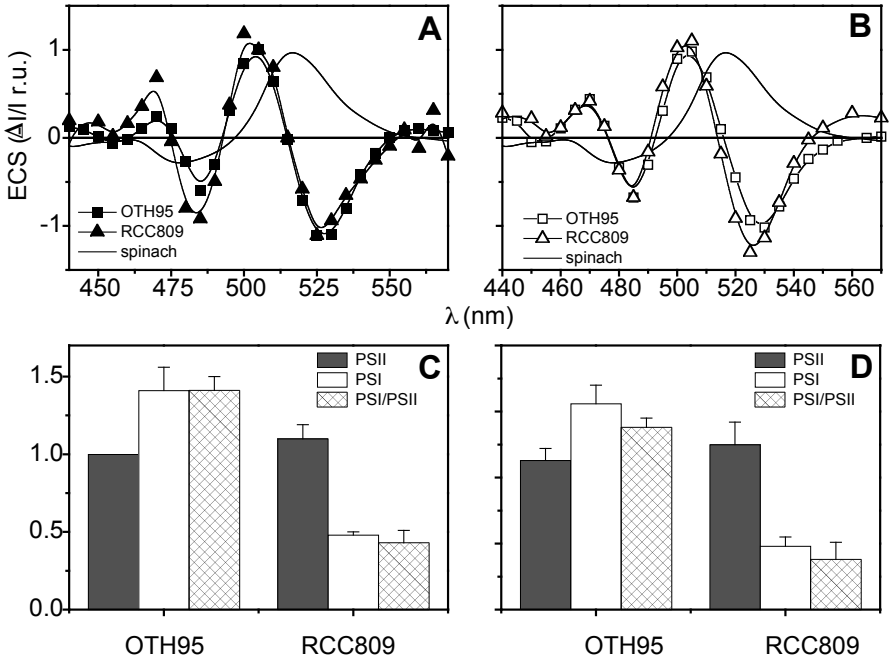


**Figure S2 online. Spectral characteristics of the electrochromic shift (ECS) and PSI/PSII ratios in OTH95 and RCC809 cells. A** and **B:** Features of the ECS signal in the OTH95 and RCC809 strains. Light absorption changes were measured 100 μs after illumination with a saturating laser flash fired at 690 nm. The ECS spectrum measured in spinach leaves (solid line) is shown for comparison. **C** and **D:** PSI and PSII charge separation capacity, as required to estimate the PSI/PSII ratios were calculated from changes in the amplitude of the fast phase of the ECS signal (at 505 nm – 525 nm) upon excitation with a saturating laser flash in presence or absence of PSII inhibitors DCMU (40 μM) and HA (1 mM) Values were normalized on Chl concentrations, and the value for PSII centers in OTH95 (100 μE $m^{-2}$ $s^{-1}$) was arbitrarily set to 1. **A** and **C**: cells were grown at 100 μE $m^{-2}$ $s^{-1}$ of white light. **B** and **D**: cells were grown at 10 μE $m^{-2}$ $s^{-1}$ of blue light.

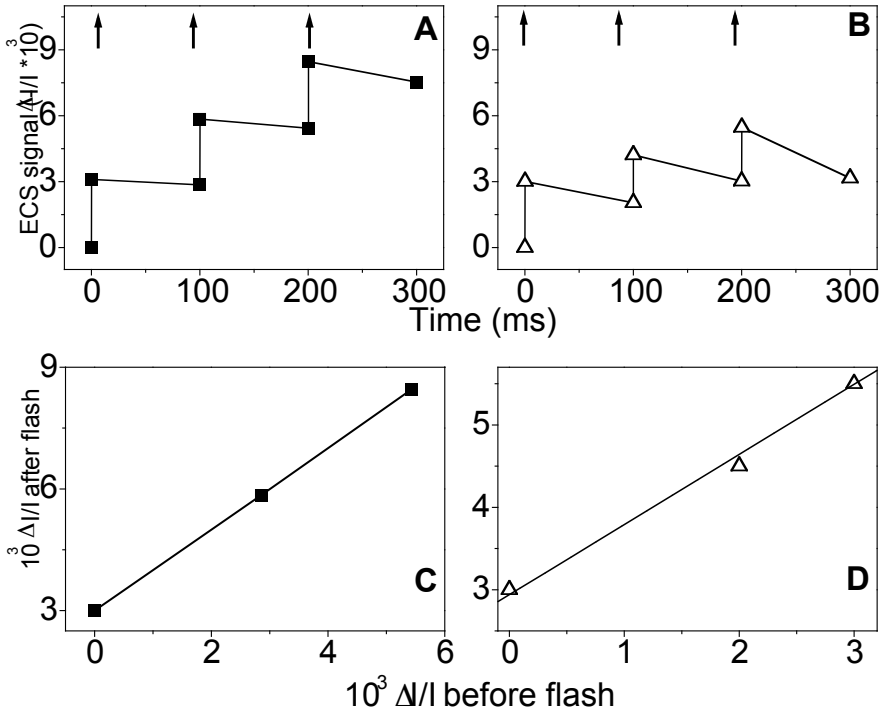


**Fig.S3 online. Photoinduced absorption changes at 505-525 nm induced in OTH95 (A, C) and RCC809 (B, D) cells by a series of 3 laser flashes fired 100 ms apart**. **A** and **B:** Absorption changes were measured 100 µs after each flash and just before the subsequent actinic flash. The dark period between two consecutive being short, a relatively small electric field dissipation occurs between two flashes. Thus the response of the ECS signal over the integrated electric field can be calculated **(C** and **D)**. Arrows: actinic flash on.

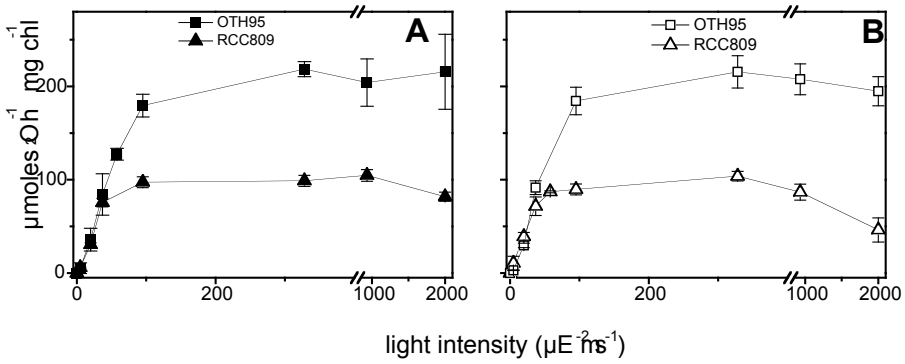


**Figure S4 online. Light saturation of oxygen evolution in OTH95 (squares) and RCC809 (triangles) cells**. Oxygen evolution and consumption were followed with a Clark electrode by increasing the light intensity every 2 min. Photosynthetic activity was calculated as "net photosynthesis" (*i.e.* photosynthesis after correction for respiration) at any given light intensity. **A**: cells were grown at 100 µE $m^{-2}$ $s^{-1}$ of white light. **B**: cells were grown at 10 µE $m^{-2}$ $s^{-1}$ of blue light. Error bars: standard error of the mean of three independent measurements.

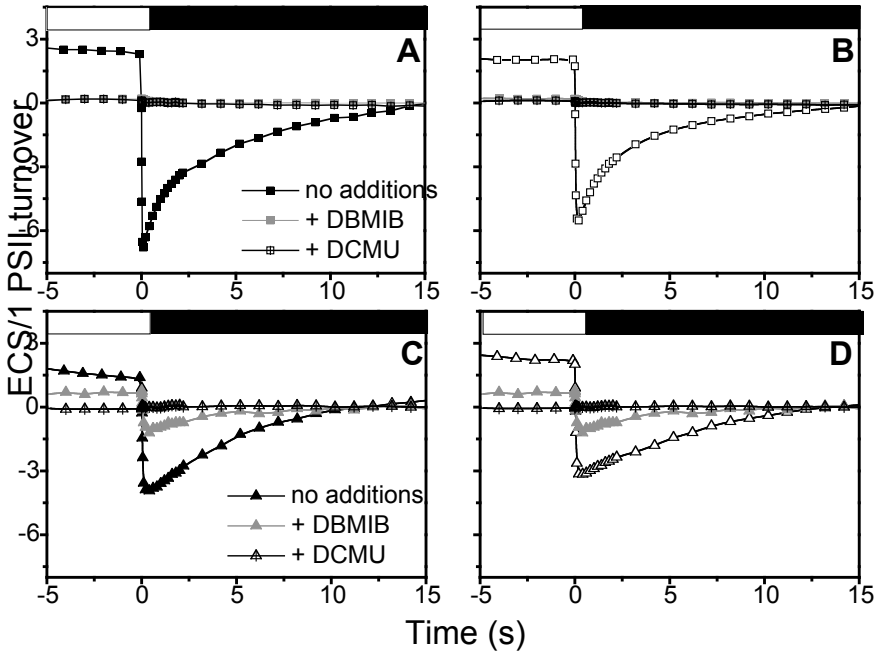


**Figure S5 online. Estimation of the electrochemical proton gradient generated upon steady-state illumination of OTH95 and RCC809 cells**. The membrane potential is evaluated by absorption changes at 505-525 nm on untreated cells (full symbols) or cells treated with 5 µM DBMIB (grey symbols) or 20 µM DCMU (crossed symbols). Samples were illuminated for 2 min with saturating light (white box). The light was then switched off (black box), and the membrane potential decay was followed until full relaxation occurred. The amplitude of the membrane potential was normalized to 1 PSII membrane charge separation, corresponding to the contribution of PSII to the signal generated by a saturating laser flash (see *e.g*. Fig. S2). **A** and **B**: OTH95. **C** and **D**: RCC809. **A** and **C**: cells were grown at 100 µE $m^{-2}$ $s^{-1}$ white light. **B** and **D**: cells were grown at 10 µE $m^{-2}$ $s^{-1}$ blue light.